Momentum Dependence of Charge Excitations in the Electron-Doped Superconductor $Nd_{1.85}Ce_{0.15}CuO_4$: a RIXS Study

K. Ishii,[1, *] K. Tsutsui,[2] Y. Endoh,[3] T. Tohyama,[2] S. Maekawa,[2] M. Hoesch,[1] K. Kuzushita,[1] M. Tsubota,[1] T. Inami,[1] J. Mizuki,[1] Y. Murakami,[1, 4] and K. Yamada[2]

[1]*Synchrotron Radiation Research Center, Japan Atomic Energy Research Institute, Hyogo 679-5148, Japan*
[2]*Institute for Materials Research, Tohoku University, Sendai 980-8577, Japan*
[3]*International Institute for Advanced Studies, Kizugawadai, Kizu, Kyoto 619-0025, Japan*
[4]*Department of Physics, Tohoku University, Sendai 980-8578, Japan*
(Dated: February 2, 2008)

We report a resonant inelastic x-ray scattering (RIXS) study of charge excitations in the electron-doped high-T_c superconductor $Nd_{1.85}Ce_{0.15}CuO_4$. The intraband and interband excitations across the Fermi energy are separated for the first time by tuning the experimental conditions properly to measure charge excitations at low energy. A dispersion relation with **q**-dependent width emerges clearly in the intraband excitation, while the intensity of the interband excitation is concentrated around 2 eV near the zone center. The experimental results are consistent with theoretical calculation of the RIXS spectra based on the Hubbard model.

The asymmetric features of the electronic phase diagram of the doping dependence of the Mott insulating Cu oxides between hole- and electron-doping have been an issue of debate for a long time. Their exploration is very important for the understanding not only of the mechanism of high-T_c superconductivity but also of the effects of doping on a Mott insulator. Experimental studies investigating the reconstruction of the electronic bands by the carrier doping have extensively been pursued [1, 2], and now the comprehension was reached that the Mott gap feature remains up to considerable doping levels. Recently angle-resolved photoemission spectroscopy (ARPES) has provided plenty of information on the momentum dependence of the occupied states [3]. On the other hand, the electronic band structure above the Fermi energy is still unclear mainly due to the lack of convincing experimental data. Electron energy loss spectroscopy (EELS) suffers from multiple scattering at large momentum transfers, while conventional optical methods, such as photo-absorption, electronic Raman scattering and so forth, can observe only the excitation at zero momentum transfer. In this respect, resonant inelastic x-ray scattering stands out as a unique and ideal probe to be able to measure the momentum dependence of the electronic excitations, in which the band structure of the unoccupied state is elucidated through the two-particle excitation spectra. Current experimental developments in the measurement of such charge dynamics or electronic excitation has been directed to the doped Mott insulators, in particular to a number of cuprates [4, 5].

The Cu K-edge RIXS experiments of the parent compounds of the high-T_c cuprates, such as $Ca_2CuO_2Cl_2$ [6] and La_2CuO_4 [7] showed a clear energy gap between the occupied lower Hubbard band (LHB), more precisely the Zhang-Rice singlet band, to the unoccupied upper Hubbard band (UHB). Recent RIXS measurements for the

hole doped cuprates showed that the Mott gap feature is robust even at considerable doping levels, besides appreciable low energy excitations corresponding to the hole doping [4, 5]. In this letter, we extended the effort to investigate the electron doped cuprates using RIXS and observe how the Mott gap feature changes with the electron doping. Combined with an extensive theoretical analysis, we can observe not only the interband excitation across the Mott gap but also the intraband excitation within the UHB throughout the whole Brillouin zone.

The RIXS experiments were carried out on the IXS spectrometer installed at the beam line 11XU of SPring-8 [8]. A Si (111) double-crystal monochromator and a Si (400) channel-cut secondary monochromator were utilized. Horizontally scattered x-rays were analyzed in energy by a bent Ge (733) crystal. The overall energy resolution is about 400 meV estimated from the full width at half maximum (FWHM) of the quasielastic scattering. Single crystals of $Nd_{2-x}Ce_xCuO_4$ of $x = 0.15$ and 0.075 were prepared, which show superconductivity below T_c = 25 K, and antiferromagnetic order below $T_N \sim 120$ K, respectively. The surface of the crystal is normal to the c-axis, which was kept in the scattering plane so as to be scanned in the reciprocal lattice space spanned by either the [100]-[001] or the [110]-[001] axes. All spectra were collected at room temperature.

Figures 1 show the incident energy (E_i) dependence of RIXS, together with the fluorescence spectra. The absolute momentum transfer is fixed at $\mathbf{Q} = (0.5, 0, 12)$. Resonantly enhanced peaks at around 2 eV and 6 eV can be seen. The latter peak was also observed in the undoped Nd_2CuO_4, and it was identified as a charge transfer excitation to the antibonding state [9]. We find two resonances at around 8990 eV and 9000 eV for the 6 eV peak. These energies correspond to the resonance energies for $\epsilon_i \parallel c$ and $\epsilon_i \parallel ab$ [10], ϵ_i being the polarization of
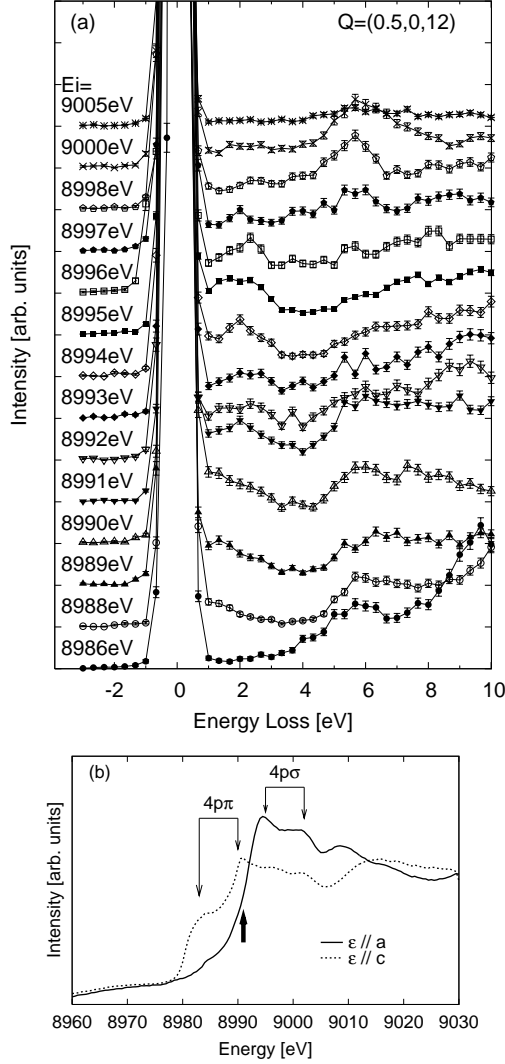
FIG. 1: (a) Resonant inelastic x-ray scattering spectra of $Nd_{1.85}Ce_{0.15}CuO_4$ as a function of energy loss at some representative incident x-ray energies E_i. The scattering vector is fixed at $\mathbf{Q} = (0.5, 0, 12)$. The strong intensity in the spectra of $E_i = 8986$ eV at high excitation energy comes from the Cu $K_{\beta 5}$ fluorescence. (b) X-ray absorption spectrum measured by the fluorescence method. The polarization of the x-rays (ϵ) is parallel to the $\mathbf{a}$- or $\mathbf{c}$-axes of the crystal. The thick arrow indicates the energy used for momentum-dependent RIXS measurements.

the incident x-ray. Because the ϵ_i is close to $\frac{\hat{\mathbf{a}} + \hat{\mathbf{c}}}{2}$ in our experimental configuration of RIXS, where $\hat{\mathbf{a}}$ and $\hat{\mathbf{c}}$ are the unit vectors along the a- and c-axes, respectively, it is reasonable that both resonances are observed. The first two peaks in the fluorescence spectra are assigned to the $1s - 4p_\pi$ transition, while the next two are the $1s - 4p_\sigma$ transition. The intensity of the 2 eV peak shows an enhancement at around 8991 eV which corresponds to the absorption edge for $4p_\sigma$. Hereafter E_i is fixed at 8991 eV to focus on the low energy excitations.

As shown in Fig. 2(a), the momentum dependence of RIXS along the c-axis is weak, as expected from the strong two-dimensionality of the CuO_2 plane. However it should be noted that the quasielastic tail is appreciably suppressed for the scan at $l = 12.5$. In our experimental condition (π-polarization of the incident x-ray), the intensity of the elastic scattering, whose major component is Thomson scattering, is mostly proportional to $\cos^2 2\theta$, where 2θ is the scattering angle and thus decreases when 2θ is close to 90 degree. It is crucially important to reduce the elastic scattering to measure the low energy excitations in RIXS. For this reason, we selected $l = 12.5$ to measure the momentum dependence in the CuO_2 plane, though it is not a high symmetry plane.

Figures 2 (b) and (c) show the momentum dependence of the RIXS spectra along a line in the $\mathbf{q} = (\pi, 0)$ and (π, π) directions, respectively, where $\mathbf{q}$ represents the reduced momentum transfer in the ab-plane. Except for the spectrum at $\mathbf{Q} = (0.75, 0, 12.5)$, all the spectra were measured at $h < 0.5$ of $\mathbf{Q} = (h, 0, 12.5)$ or $\mathbf{Q} = (h, h, 12.5)$. The spectrum at $\mathbf{Q} = (0.75, 0, 12.5)$ lies between those of $\mathbf{Q} = (0.2, 0, 12.5)$ and $\mathbf{Q} = (0.3, 0, 12.5)$, which indicates that the electronic structure is symmetric with respect to $h = 0.5$. In order to examine the momentum dependence more clearly, we subtract the elastic contribution near 0 eV and the high-energy contribution above 4 eV from the raw data (dashed lines in Figs. 2(b) and (c)). The former is estimated from the anti-Stokes region, and the latter is treated as a tail of the excitation at 6 eV by extrapolating smoothly to the lower-energy region. The open symbols in Figs. 2(b) and (c) are the resulting spectra, where the data below 0.6 eV are not shown due to the uncertainty in the assignment of the quasielastic contributions. The spectra are replotted in Fig. 2(d) as a contour map, where the maximum intensity at each momentum point is normalized to unity and a smoothing procedure is applied. We can clearly see two characteristic excitations. One is the excitation at 2 eV observed at the zone center. Its intensity rapidly decreases with increasing $\mathbf{q}$. The other one is a broad but dispersive excitation along the $(\pi, 0)$ and (π, π) directions. As a function of $|\mathbf{q}|$, the latter excitation shifts to higher energy up to 2-2.5 eV at the zone boundary, accompanied by an increase of the spectral width. The upper edges of the excitations are dispersive with a width of more than 2 eV from the zone center to the zone boundary.

Two characteristic excitations just described above have been elucidated further by duplicating the similar scans for $x = 0.075$ crystal. Typical data of scans are shown in Fig. 2(e). The excitation spectra at the zone center superpose each other and it is essentially independent of x. On the other hand, the spectra at finite $\mathbf{q}$s show the weaker intensities for $x = 0.075$ in lower-energy region and the intensity seems to be proportional to x. Such dependence on doping indicates different nature between two excitations which is identified by the follow-
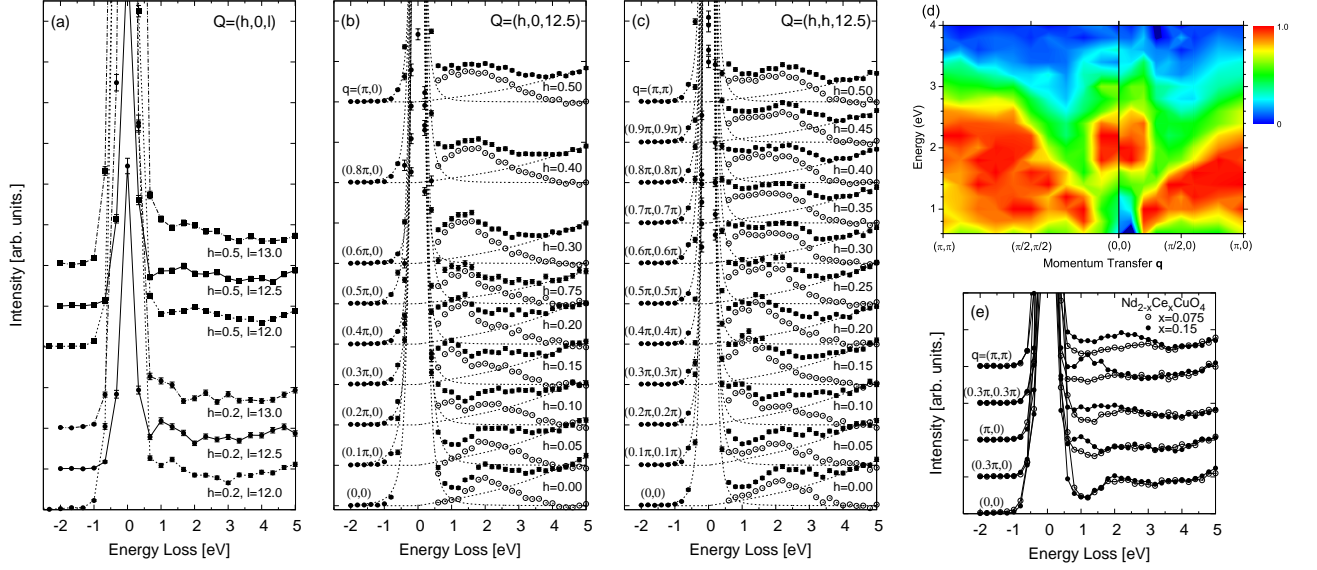
FIG. 2: Momentum dependence in $Nd_{1.85}Ce_{0.15}CuO_4$. (a) Along the c-axis, (b) $(\pi,0)$, and (c) (π,π) directions. $E_i = 8991$ eV. The filled symbols are raw data, and the open ones in (b) and (c) are data from which the elastic scattering and the scattering at higher energy (dotted lines) are subtracted. (d) Contour plot of the RIXS intensity. After subtraction of the elastic and high-energy contributions (open symbols in (b) and (c)) the data are normalized for the maximum intensity in each momentum and interpolated smoothly. (e) Comparison of the RIXS spectra to $Nd_{1.925}Ce_{0.075}CuO_4$.

ing theoretical analysis of RIXS from the electron-doped CuO_2 plane.

Keeping in mind the nearly monotonic dispersion like excitation mode, we performed calculations of the RIXS spectrum using the numerically exact diagonalization technique on a 4×4 cluster of a Hubbard model with the electron density $18/16 = 1.125$. The model includes the hopping of the electrons between first, second, and third nearest neighbor sites (t, t', and t'', respectively) and the on-site Coulomb interaction U. The RIXS spectrum is expressed as a second-order process of the dipole-transition between Cu $1s$ and $4p$ orbitals, where a Coulomb interaction between a $1s$ core-hole and a $3d$ electron, U_c, is explicitly included [11]. We use $t'/t = -0.25$ and $t''/t = 0.12$, which are obtained from shape of the Fermi surface [12]. For other parameters, we take $U/t = 8$, $U_c/t = 10$, and $t = 0.3$ eV. The inverse of the life time of the intermediate state is assumed to be $\Gamma = 3t$.

Figure 3 shows the calculated RIXS spectrum, where E_i is set to a value denoted by the arrow in the absorption spectrum shown in the inset. The RIXS spectrum shows two characteristic excitations similar to the observed ones: One is a 2 eV excitation at $\mathbf{q} = (0,0)$, and the other is a broad band of excitations up to ~ 3 eV for all momenta except $(0,0)$. The 2eV excitation is the Mott gap excitation from LHB to UHB, as discussed in Ref. [13]. The broad excitations can be assigned to the intraband excitation. To confirm this, we calculated the dynamical density response function $N(\mathbf{q},\omega)$,

which can describe the momentum-dependent intraband and interband density fluctuations separately when U is large [14, 15, 16, 17, 18]. Comparing RIXS and $N(\mathbf{q},\omega)$ (broken lines), we find qualitatively similar behavior for all momentum and energy regions except for the 2 eV excitation at $\mathbf{q} = (0,0)$. This means that the broad and dispersive excitations observed in Fig. 2 come from the charge fluctuations in the metallic phase.

The energy position of the highest peak in RIXS and $N(\mathbf{q},\omega)$ is plotted in the inset of the right panel of Fig. 3. In addition to the positions taken from the main panels, we plot peak positions obtained from a $\sqrt{18} \times \sqrt{18}$ cluster with an electron density $20/18$. The resulting momentum dependence is found to trace out the center the of broad spectra in the contour plot of Fig. 2(d). This agreement justifies the assignment of the observed two structures to the Mott-gap and intraband excitations.

As emphasized above, the intraband excitations show broad features. Such a broadness comes from strong correlation common to Hubbard-type models [14, 15, 16, 17, 18], and thus it is independent of the presence of the long-range hoppings. Instead, the effect of t' and t'' may appear in the very low-energy region, where excitations are predominately controlled by the Fermi surface topology inducing $2k_F$ and $4k_F$ branches [14], k_F being the Fermi momentum. Unfortunately, at present the energy resolution of RIXS is limited so that it is difficult to resolve the branches. We continue our efforts to improve the energy resolution and this will open a new view of the intraband charge excitations in the high-T_c cuprates
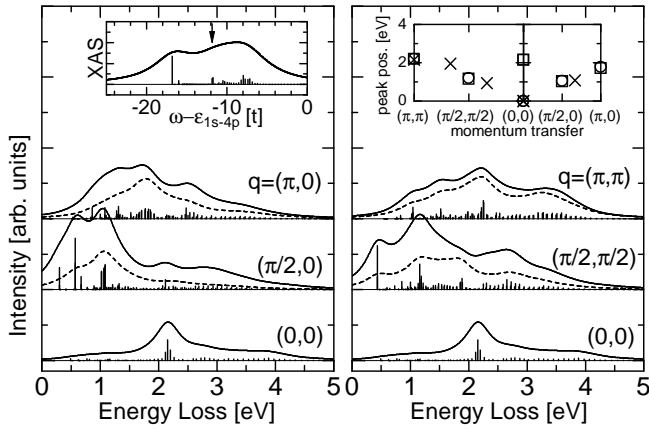
FIG. 3: The RIXS spectrum of an electron-doped 4×4 Hubbard cluster with long-range hopping terms. The electron density is $18/16 = 1.125$, and the model parameters are $t'/t = -0.25$, $t''/t = 0.12$, $U/t = 8$, $U_c/t = 10$, and $\Gamma/t = 3$ with $t = 0.3$ eV. The δ-functions are convoluted with a Lorentzian broadening of $0.8t$. Broken lines: $N(\mathbf{q}, \omega)$ for the same cluster. The inset of the left panel: the calculated absorption spectrum with a Lorentzian broadening of $3t$. The vertical arrow denotes E_i for RIXS. The inset of the right panel: momentum dependence of the peak positions of RIXS (the squares), together with those of $N(\mathbf{q}, \omega)$ for 4×4 (the circles) and $\sqrt{18} \times \sqrt{18}$ (the crosses) clusters.

in the future.

Although we made use of electron-doped $Nd_{1.85}Ce_{0.15}CuO_4$, it may also be possible to use hole-doped materials such as $La_{2-x}Sr_xCuO_4$ to detect the intraband excitation. However, it is important to notice that there is an advantage of electron doping over hole doping. As seen in the inset of the left panel of Fig. 3, the absorption spectrum shows three components: $\omega - \epsilon_{1s-4p} = -17t$, $-12t$, and $-8t$. The latter two components are also seen in the undoped system. On the other hand, the former appears upon electron doping only, corresponding to a final state where the core hole attracts a doped electron on the same site. Therefore, the final state hardly contains any pair of empty and doubly occupied sites, i.e., no excitations across the Mott gap. This means that, the intraband charge excitations dominate the RIXS spectrum if E_i is tuned to the lowest-energy peak. As long as we fix E_i to the absorption-edge region, the contribution from the lowest-energy peak induces large intraband charge excitations. In our case we select the incident energy to the absorption edge for $4p_\sigma$ as shown in Fig. 1(b), and this condition is satisfied. In contrast, a corresponding final state in the hole-doped system, which emerges after hole doping, exists in a much higher-energy region at around $\omega - \epsilon_{1s-4p} = 0$ [13]. Experimentally tuning the incident photon energy to this region seems to be difficult because of the overlap of other absorption processes.

Finally, we compare the interband excitations across the Mott gap between hole- and electron-doping. Recently RIXS experiments for $La_{2-x}Sr_xCuO_4$ have been reported [4, 5]. Their results showed that the spectral shape is almost independent of the momentum transfer except for small shifts in energy. On the other hand, the interband excitation of $Nd_{1.85}Ce_{0.15}CuO_4$ concentrates on a energy (~ 2 eV) at the zone center and becomes broad in energy with increasing momentum transfer. Such a difference in momentum dependence is consistent with a previous theoretical result [13], where the difference in the strength of antiferromagnetic correlation plays a crucial role.

In summary, we have performed a RIXS study for the electron-doped superconductor $Nd_{1.85}Ce_{0.15}CuO_4$, and found characteristics of the intraband and interband excitations. The intraband excitation shifts to higher energy with the increase of the peak width as a function of momentum transfer. The spectral shape of the intraband excitation has a similarity to $N(\mathbf{q}, \omega)$ of the two-dimensional Hubbard model. This demonstrates that RIXS is a good tool to measure momentum-dependent density fluctuations in strongly correlated metallic systems. On the other hand, the interband excitation across the Mott gap is enhanced in intensity at the zone center, which is in contrast to the momentum-independent spectral shape in hole-doped $La_{2-x}Sr_xCuO_4$.

* Electronic address: kenji@spring8.or.jp
[1] S. Uchida, et al., Phys. Rev. B **43**, 7942 (1991).
[2] Y. Onose, et al., Phys. Rev. B **69**, 024504 (2004).
[3] A. Damascelli, Z. Hussain, and Z.-X. Shen, Rev. Mod. Phys. **75**, 473 (2003).
[4] Y.-J. Kim, et al., Phys. Rev. B **70**, 094524 (2004).
[5] M. Z. Hasan, et al., cond-mat/0406654.
[6] M. Z. Hasan, et al., Science **288**, 1811 (2000).
[7] Y. J. Kim, et al., Phys. Rev. Lett. **89**, 177003 (2002).
[8] T. Inami, et al., Nucl. Inst. & Mech. in Phys. Res. A **467-468**, 1081 (2001).
[9] J. P. Hill, et al., Phys. Rev. Lett. **80**, 4967 (1998).
[10] K. Hämäläinen, et al., Phys. Rev. B **61**, 1836 (2000).
[11] K. Tsutsui, T. Tohyama, and S. Maekawa, Phys. Rev. Lett. **83**, 3705 (1999).
[12] N. P. Armitage, et al., Phy. Rev. Lett. **87**, 147003 (2001).
[13] K. Tsutsui, T. Tohyama, and S. Maekawa, Phys. Rev.

Lett. **91**, 117001 (2003).

[14] T. Tohyama, P. Horsch, and S. Maekawa, Phys. Rev. Lett. **74**, 980 (1995).

[15] R. Eder, Y. Ohta, and S. Maekawa, Phys. Rev. Lett. **74**, 5124 (1995).

[16] G. Khaliullin and P. Horsch, Phys. Rev. B **54**, R9600 (1996).

[17] D. H. Kim, D. K. K. Lee, and P. A. Lee, Phys. Rev. B **55**, 591 (1997).

[18] C. Gröber, R. Eder, and W. Hanke, Phys. Rev. B **62**, 4336 (2000).